

See discussions, stats, and author profiles for this publication at: <https://www.researchgate.net/publication/279193280>

# The influence of localized plasmons on the optical properties of Au/ZnO nanostructures †

Article in *Journal of Materials Chemistry C* · May 2015

DOI: 10.1039/c5tc00964b

CITATIONS

37

READS

626

14 authors, including:



**Roman Viter**

University of Latvia

111 PUBLICATIONS 1,420 CITATIONS

[SEE PROFILE](#)



**Zigmas Balevicius**

Center for Physical Sciences and Technology

45 PUBLICATIONS 721 CITATIONS

[SEE PROFILE](#)



**Adib Abou Chaaya**

Lebanese University

29 PUBLICATIONS 721 CITATIONS

[SEE PROFILE](#)



**Ieva Baleviciute Plikusiene**

Vilnius University

27 PUBLICATIONS 608 CITATIONS

[SEE PROFILE](#)

Some of the authors of this publication are also working on these related projects:



Nanomaterials for Photocatalysis [View project](#)



Nanoelectromechanical systems [View project](#)



CrossMark  
click for updates

Cite this: *J. Mater. Chem. C*, 2015, **3**, 6815

## The influence of localized plasmons on the optical properties of Au/ZnO nanostructures†

R. Viter,<sup>\*ab</sup> Z. Balevicius,<sup>cd</sup> A. Abou Chaaya,<sup>e</sup> I. Baleviciute,<sup>cf</sup> S. Tumenas,<sup>c</sup> L. Mikoliunaite,<sup>cf</sup> A. Ramanavicius,<sup>cf</sup> Z. Gertnerė,<sup>g</sup> A. Zalesska,<sup>a</sup> V. Vataman,<sup>a</sup> V. Smyntyna,<sup>a</sup> D. Ertė,<sup>g</sup> P. Miele<sup>e</sup> and M. Bechelany<sup>\*e</sup>

Optical and structural experiments have been carried out on Si/ZnO thin films modified with ultra-thin gold layers of different thicknesses. ZnO was produced via Atomic Layer Deposition (ALD) and Au via Physical Vapor Deposition (sputtering). The structural properties of nanostructures were studied by XRD and AFM. Optical characterization was performed by absorbance, photoluminescence (PL) and spectroscopic ellipsometry (SE). A transition from cluster-to-thin films with the increase of Au thickness has been revealed from an analysis of optical and structural parameters. The analysis of optical features of the system has shown that slight changes of the localized plasmon absorption peaks in spectra make a significant contribution to complex refractive index of gold film and, as a result, leads to a strong enhancement of UV PL peak in the ZnO layer. The mechanism of the tailoring of ZnO optical features changes by varying the Au layer thickness was discussed. Our studies have shown that through the changes of structural properties of thin gold layer between the Si substrate and the ZnO film, we can tune the optical dispersion of each layer and hence the control of ZnO PL spectra enhancement and quenching in UV-Vis wavelengths region is possible. In order to apply the hybrid structure under consideration in various optical applications, such as LED, the dispersion of the complex refractive index of the components should be optimized taking into account a particular target.

Received 6th April 2015,  
Accepted 22nd May 2015

DOI: 10.1039/c5tc00964b

www.rsc.org/MaterialsC

## A Introduction

Zinc oxide (ZnO) is a promising material for various optical applications, like LED, optical coatings, gas sensors<sup>1</sup> and biosensors.<sup>2–6</sup> Being an n-type semiconductor with a band gap of around 3.3 eV, it demonstrates high exciton binding energy (0.06 eV) and strong emission bands in both UV and Vis wavelength ranges, which is caused by near band and defect level emissions, correspondingly.<sup>7</sup> The optical and structural parameters of ZnO can be tailored by

varying its layer deposition conditions and/or doping of formed structures.<sup>7,8</sup>

Ultrathin metal layers and nanoparticles (*e.g.* Au, Ag, Cu, *etc.*), which are able to generate localized surface plasmon resonance,<sup>9–11</sup> resulted in an optical absorption peak in the visible range. The peak position strongly depends on the structure of the layer or the size of the particles and the surrounding media.<sup>12–14</sup> Gold-based templates could be used to control the growth of ZnO.<sup>15,16</sup> It was found that gold nanoclusters supported the growth of ZnO nanowires from ZnO nanoparticles<sup>16</sup> and gold microspheres were used as support for single ZnO nanowire growth.<sup>15</sup> In addition, a lot of studies have been dedicated to the synthesis and the study of the optical properties of ZnO/Au heterostructures, by depositing gold on ZnO nanostructures using different techniques such as the attachment of Au-capped nanoparticles,<sup>17–19</sup> sputtering,<sup>20,21</sup> microwave-assisted chemical synthesis,<sup>22</sup> and *in situ* photochemical metal-deposition.<sup>23</sup> It was shown that gold nanostructures can tune the structural and optical properties of ZnO nanostructures.

Most of above mentioned applications required the enhancement of the photoluminescence of ZnO in the UV range. Localized surface plasmon resonance of thin gold nanolayers has been widely used for the enhancement of PL in ZnO layers.<sup>21,24</sup> The structure of the thin gold films strongly influences the

<sup>a</sup> Faculty of Physics, Experimental Physics Department, Odessa National I.I. Mechnikov University, 42, Pastera, 65026, Odessa, Ukraine.  
E-mail: viter\_r@mail.ru; Tel: +380676639327

<sup>b</sup> Institute of Atomic Physics and Spectroscopy, University of Latvia, 19, Raina Blvd., LV 1586, Riga, Latvia

<sup>c</sup> State Research Institute Center for Physical Sciences and Technology, Savanoriu ave. 231, LT-01108, Vilnius, Lithuania

<sup>d</sup> Faculty of Electronics, Vilnius Gediminas Technical University, Sauletekio 11, LT-10223, Vilnius, Lithuania

<sup>e</sup> Institut Européen des Membranes, UMR 5635 ENSCM UM CNRS, Université Montpellier, Place Eugene Bataillon, F-34095 Montpellier Cedex 5, France

<sup>f</sup> Faculty of Chemistry, Department of Physical Chemistry, Vilnius University, Naugarduko 24, 03225 Vilnius 6, Lithuania

<sup>g</sup> Institute of Chemical Physics, University of Latvia, 19, Raina Blvd., LV 1586, Riga, Latvia

† Electronic supplementary information (ESI) available. See DOI: 10.1039/c5tc00964b

dispersion of the refractive index and extinction coefficient of such nanostructures, and as a result, the enhancement efficiency of PL spectra in ZnO. This is the reason why the optical response of ultrathin metal films is of special interest and should be analyzed in more detail, in particular in complex Au/ZnO nanostructures.

In this paper we report the formation of Au–ZnO nanostructures on a Si substrate using two original methods of deposition of thin films: atomic layer deposition (ALD) and magnetron sputtering techniques. Structural properties of nanostructures were studied using XRD and AFM. Optical characterization was performed by absorption measurements and photoluminescence (PL). Special attention was paid to the determination of the dispersion of refractive index and extinction coefficient of gold nanolayers and ZnO films by spectroscopic ellipsometry (SE). The large interface sensitivity of SE enables us to analyze in detail, the optical properties of ultrathin layers.<sup>25</sup> The aim of this work was dual. Firstly, SE has been utilized to demonstrate the influence of thin gold sublayer structures on the growth and optical constants of ZnO layers and secondly, to reveal the contribution of the localized surface plasmon resonance (LSPR) effect to the optical dispersion of gold layers and, as a result, to the efficiency of ZnO PL spectra in the UV-Vis range.

## B Materials and methods

### 1. Materials

Diethyl zinc (DEZ) ( $\text{Zn}(\text{CH}_2\text{CH}_3)_2$ , 95% purity, CAS: 557-20-0) was purchased from Sigma Aldrich. Silicon wafer p-type (100) was obtained from MEMC Korea company and glass substrates from RS France.

### 2. Synthesis of Au/ZnO nanostructures by ALD/PVD

Substrates were pre-cleaned in acetone, ethanol and deionized water for 5 min to remove organic contaminants. A custom-made ALD reactor was used for the synthesis of ZnO.<sup>7</sup> ALD was performed using sequential exposures of DEZ and  $\text{H}_2\text{O}$  separated by a purge of Argon with a flow rate of 100 sccm. The deposition regime for ZnO consisted of 0.1 s pulse of DEZ, 30 s of exposure to DEZ, 30 s of purge with Argon followed by 2 s pulse of  $\text{H}_2\text{O}$ , 30 s of exposure to  $\text{H}_2\text{O}$  and finally 40 s purge with Argon. ZnO thin films were deposited both on Si substrates and glass substrates by ALD, the temperature being fixed to 100 °C. The growth rate was typically 2 Å per cycle for ZnO.<sup>7,26</sup>

Gold coating was performed using sputtering (Edwards Scancoat Six) in an argon plasma discharge. The operating conditions were as follows: working pressure  $10^{-1}$  mbar, voltage 1.7 kV, substrate temperature close to 20 °C, and current 10 mA. The deposition time was adjusted to get the desired thickness of gold.<sup>27</sup>

Thin ZnO–Au nanostructures were obtained: the Au layer was deposited on the substrate and then coated with a ZnO layer. The thickness of ZnO was 50 nm and was kept constant for all depositions. The Au thickness varied from 2.5 nm to 30 nm.

## 3. Characterization

The structural properties were characterized by X-ray diffraction (PANalyticalXpert-PRO diffractometer equipped with a X'celerator detector using Ni-filtered Cu-radiation). The surface morphology was studied using a Asylum Research MFP-3D Atomic Force Microscope, operated in tapping mode and equipped with a commercial silicon tip. The size of the AFM images was  $3 \mu\text{m} \times 3 \mu\text{m}$ .

The optical properties of the samples have been studied with absorption measurements, photoluminescence spectroscopy and spectroscopic ellipsometry. In order to characterize the optical response of Au/ZnO nanostructures a UV-Vis spectrophotometer Shimadzu UV-3600 was used to measure absorbance spectra of the samples in the range of 300–850 nm. The measurement was performed employing an integrating sphere of 60 mm diameter to account for a possible scattering from nanostructures.

The photoluminescence (PL) spectra of the samples were measured at room temperature using a custom-made setup.<sup>28</sup> Excitation of PL has been achieved using a solid state laser (355 nm) and the emission spectra were recorded in the range 360–800 nm.<sup>28</sup>

Spectroscopic ellipsometry measurements have been performed in order to determine the dispersion of refractive index and extinction coefficient of various thicknesses of gold and 50 nm ZnO layers. Ellipsometric measurements have been carried out in the spectral range from 300 nm to 1000 nm and angle of incidence of 75° degrees. Curves of optical dispersion of the Au, Au/ZnO films on Si substrate were obtained employing J.A. Woollam M2000X spectroscopic ellipsometer with rotating compensator. The experimental ellipsometric data were analyzed by means of the J.A. Woollam program CompleteEase.

## C Results and discussion

### 1. Chemical and structural characterizations

In order to study the influence of Au thickness on the properties of the ZnO ALD film, six different samples have been elaborated and fully characterized. The crystal quality of ZnO and Au films were analyzed by XRD. Fig. 1 shows XRD spectra of the obtained samples. It was found that the samples with the thinnest Au layers in the range of 2.5–10 nm showed a low intensity peak at  $2\theta = 37.8^\circ$ , related to (111) of Au phase, pointing to the poor crystalline/amorphous structure of gold. The increase of thickness of Au films (15 and 30 nm) led to the appearance of the XRD peaks at  $2\theta = 38.7^\circ$ .

A low and wide peak at  $2\theta = 34.2^\circ$ , related to (002) of ZnO phase, was observed when ZnO 50 nm film was grown *via* ALD on Au layers with 2.5 to 10 nm thick. Significant increase of the peak intensity is observed for Au and ZnO reflections when the thickness of Au is increased to 15 nm in the Au–ZnO composition. From XRD data analysis of Au–ZnO nanostructures, the shift of the peak position towards higher values of  $2\theta$  and the decrease of full width at half maximum (FWHM) of the peaks, related to ZnO were observed with an increase of the Au layer thickness.

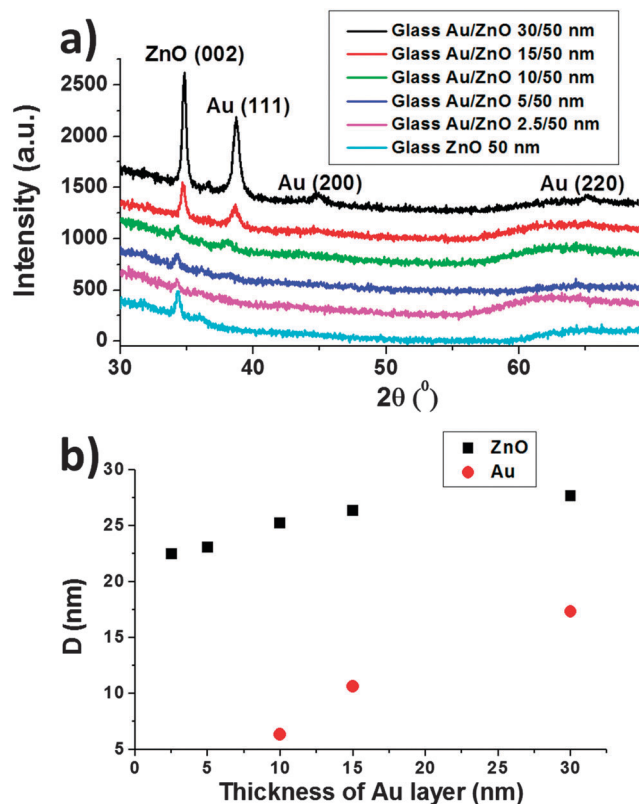


Fig. 1 (a) XRD spectra of Au–ZnO nanostructures with different thicknesses of Au; (b) grain size of ZnO and Au nanostructures vs. Au nanolayer thickness.

The grain size  $D$  of ZnO and Au nanolayers was calculated using Scherrer's equation:<sup>7,29</sup>

$$D = \frac{0.9\lambda}{\beta \cos(\theta)} \quad (1)$$

where  $\lambda = 0.154$  nm (X-ray wavelength),  $\theta$  is the diffraction angle and  $\beta$  is the half maximum (FWHM).

The wide and the low intense XRD reflections for 2.5 and 5 nm thick Au films point to a grain size lower than 4 nm and a cluster–cluster like structure of the Au films. The grain size of Au increased with the thickness of the layer. The grain size dependence on Au layer thickness is summarized in Fig. 1b for bare Au nanolayers and ZnO layers in Au–ZnO nanostructures. A significant increase of the grain size of Au-based layers was observed with the increase of layer thickness. The grain size of ZnO layers increased by 10–15% and it became steady when the Au sublayer thickness reached 30 nm.

The surface morphology of Au layers was characterized by atomic force microscopy (AFM) (Fig. S11, ESI†). The investigated samples consisted of well-shaped crystallites with an average size of ~20–30 nm. Morphology studies have shown that surface roughness of Au films with thickness in the range of 2.5 to 10 nm differed significantly from samples with Au thickness for 15 and 30 nm. The surface roughness rapidly decreased and became quasi saturated for the samples with Au thickness 15 and 30 nm. The RMS-values of surface roughness were 2.86, 3,

4.51, 2.46 and 2.5 nm for Au films with increasing film thickness, respectively (Fig. S12, ESI†).

## 2. Absorbance spectra

The absorption spectra of the Au nanostructures, deposited on glass, of thicknesses ranging from 2.5 to 30 nm are recorded in the wavelength range of 300–850 nm and the reflectivity spectra is presented in the ESI† (Fig. S13). The red shift and broadening of a localized plasmon band (500–650 nm) increase with an increase of the thickness from 2.5 to 15 nm. The absorption spectra of composite Au–ZnO nanostructures with different Au thicknesses are presented in Fig. 2. The spectra of Au–ZnO samples clearly show two peaks. The first peak is located in the visible region at about 570 nm and it is related to surface plasmon absorption. As is the case in the bare Au nanostructures, the surface plasmon peak shows red shift and broadens with the increase of Au thickness from 2.5 to 15 nm. Surface plasmon absorption does not manifest in nanostructures with Au layers of 30 nm. The second peak is located in the ultraviolet region at about 380 nm and it is related to the near band edge absorption of ZnO.

## 3. Spectroscopic ellipsometry studies

Spectroscopic ellipsometry measurements have been performed in order to determine the influence of optical dispersion features of various gold layers thicknesses on the optical response of Si/Au/ZnO nanostructures.

The optical response of ellipsometric parameters for pure gold layers showed that the localized plasmon absorption manifesting themselves as the dip in the spectra of  $\Psi(\lambda)$  and  $\Delta(\lambda)$  were excited at about 520 nm for 2.5–15 nm thick Au layer at external angles of light incidence equal to 70 degrees. Meanwhile, for the sample of Si/Au with gold thickness of 30 nm, localized plasmons are not observed and the optical response of ellipsometric parameters was more like that of bulk gold (J.A. Woollam CompleteEASE database, version 4.13).

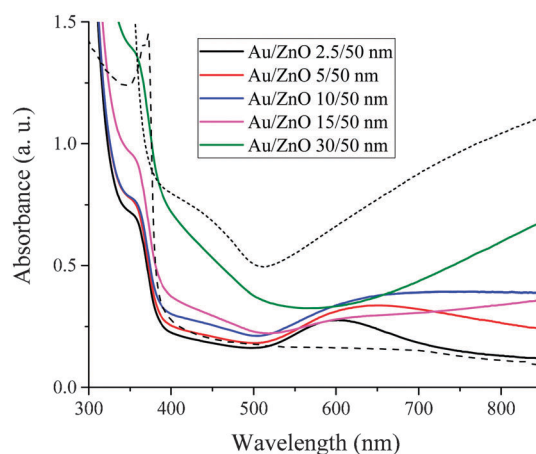


Fig. 2 UV-Vis absorption spectra of Au–ZnO nanostructures with different Au thicknesses. Dashed and dotted curves present, for a comparison absorption spectra of pure ZnO (thickness ~100 nm) and Au (~50 nm).

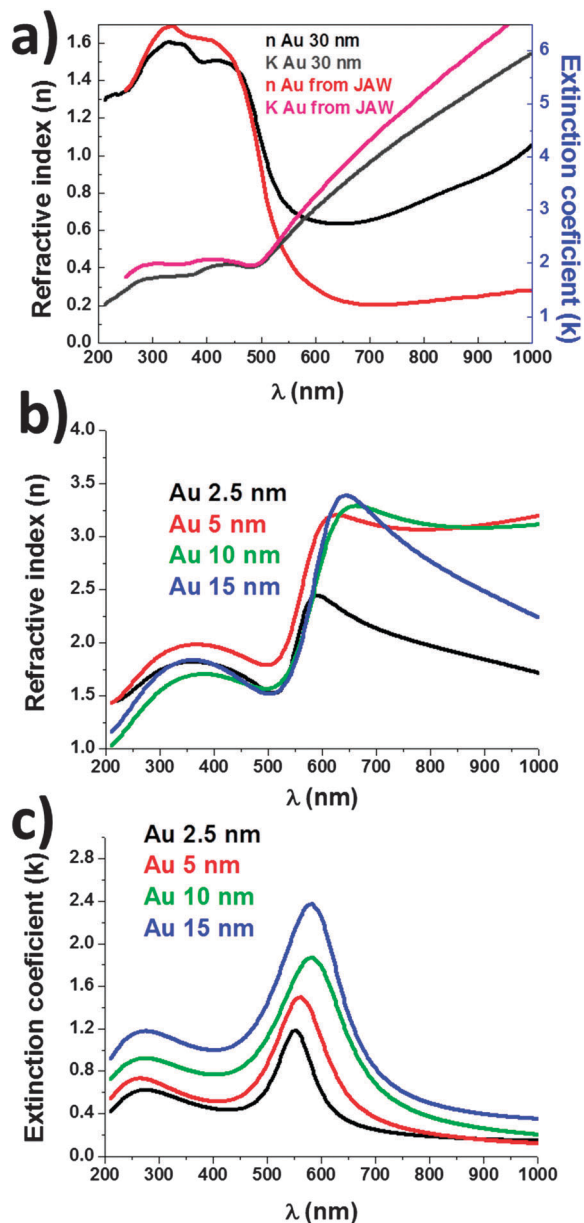


Fig. 3 Complex refractive index of 30 nm Au film compared to reference data (J.A. Woollam CompleteEASE database, version 4.13) (a); spectra of real ( $n$ ) (b) and imaginary ( $k$ ) parts (c) of refraction index of Au island-like films (2.5–15 nm) obtained from analysis of ellipsometric data in multilayer model.

In order to model the spectral dependence of ellipsometric parameters of pure Au island-like films, the contributions of Drude function and Lorentz oscillators were taken into account.<sup>30,31</sup> The calculated ellipsometric spectra for island-like Au layers (2.5–15 nm thick) on the Si substrate were fitted to experimental data, accepting as adjustable parameters the constants in the dispersion due to the localized plasmon absorption (two Lorentz terms). The contribution of Lorentz oscillators was enough to achieve a reasonable agreement between calculated and experimental data for Si substrate/Au island-like films. The dispersion of the refractive index for the Au film determined from the fitting procedure of ellipsometric data for the sample

Si substrate/Au 30 nm is presented in Fig. 3a and compared to reference data (J.A. Woollam CompleteEASE database, version 4.13).

Analysis of ellipsometric data, which have been obtained on the hybrid structure with 50 nm thick ZnO films on the top of Au island-like layers, was performed in a multilayer model using an analogous fitting procedure to that for the Si/Au samples. The dispersion of Au island-like films determined for the Si/Au samples was used as a starting point in the fitting procedure for the Si/Au with additional ZnO 50 nm thick films. Regression analysis has shown that the dispersion of the refractive index and the extinction coefficient of Au island-like films had the same shape (Lorentz type) as in the case of Si/Au samples (Fig. 4a–c). A small shift of the localized plasmon peak to longer wavelengths can be caused by the presence of

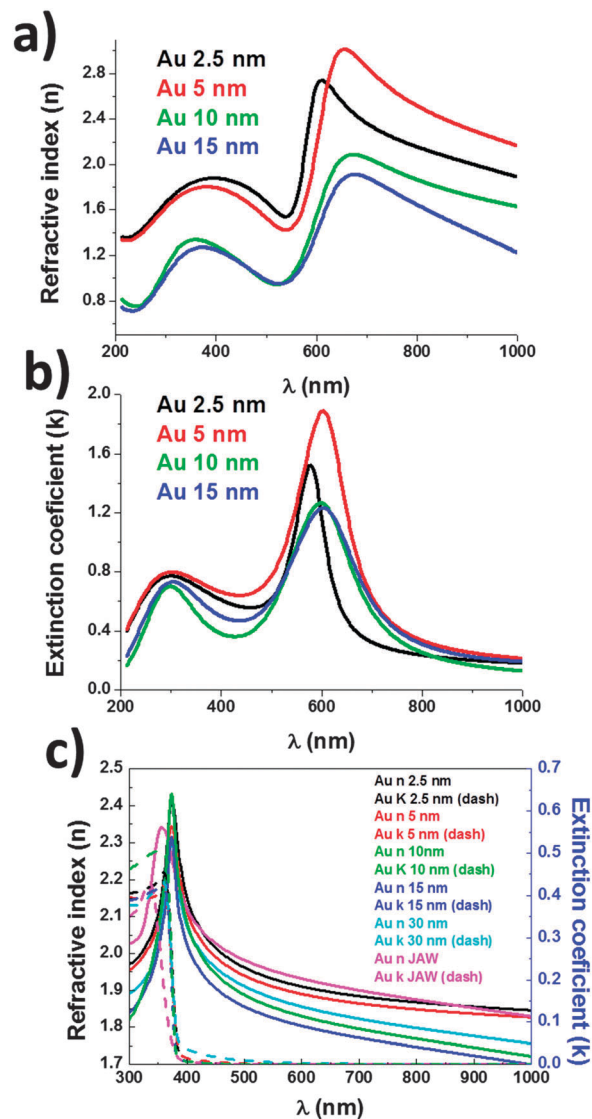


Fig. 4 Spectra of real ( $n$ ) (a) and imaginary ( $k$ ) parts (b) of complex refractive index of Au island-like films for structure Si/Au/ZnO obtained from analysis of ellipsometric data in multilayer model. (c) Spectra of real ( $n$ ) and imaginary ( $k$ ) parts of refraction index of ZnO 50 nm films for multi-layered nanostructure of Si substrate/Au (2.5–30 nm)/ZnO 50 nm.

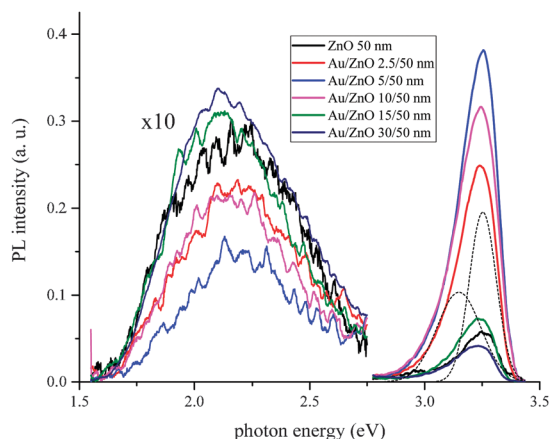


Fig. 5 Room temperature photoluminescence spectra of Au/ZnO nanostructures. Dashed curves presents decomposition of the main excitonic peak of Au/ZnO (2.5/50 nm) nanostructure.

the ZnO layer on the top of the gold films. Meanwhile, in order to model the optical constants of 50 nm thick ZnO films, the PSEMI-M0 function and two Gaussian oscillators as starting parameters have been taken from J.A. Woollam software CompleteEase.

**Photoluminescence spectra.** Room temperature photoluminescence spectra of Au/ZnO nanostructures are shown in Fig. 5. The spectra clearly exhibit two main optical features, one in the UV region, located at 3.26 eV, and the second in the Vis region at about 2.1 eV. The first peak is related to ZnO near-band-edge excitons and the second one is related to a deep-level emission. For the Au/ZnO (5/50 nm) nanostructure, the UV emission of 3.26 eV is evidently enhanced while the visible emission is reduced. For the Au/ZnO (30/50 nm) nanostructure, in contrast, the UV emission is quenched and the visible peak of 2.1 eV is increased. For the Au/ZnO (5/50 nm) nanostructure, the UV emission intensity is larger by a factor of  $\sim 10$  compared to the intensity of the 30/50 nm nanostructure, while the Vis emission is decreased by a factor of  $\sim 2.5$  with respect to the 30/50 nm nanostructure. The PL spectra were analyzed using the Gaussian function. The decomposition of the excitonic peak is presented by dashed curves for the Au/ZnO (2.5/50 nm) sample in Fig. 5.

## D Discussion

It is reasonable to assume that ultra-thin gold layers demonstrate different crystalline structures and surface roughness influenced by their thicknesses.<sup>32,33</sup> As noted above, gold nanolayers with a thickness between 2.5 and 10 nm have shown cluster-like structures with grain sizes lower than 3–4 nm, which was confirmed by XRD data and higher surface roughness profiles evaluated from AFM micrographs (Fig. S1, ESI†). Meanwhile, the increase of the XRD peak intensity and its narrowing for 15 and 30 nm Au layers demonstrate the improvement of the crystalline structure of Au layers. Decrease of the surface roughness values for Au nanolayers in the range of 15–30 nm indicates the transition to a bulk-like structure. Therefore, the deposition of ZnO layers on the top of gold

sub-layers can change the structural parameters of the ZnO films.<sup>12,34</sup> Assuming that the different structures of ultra-thin gold layers strongly influence the deposition process of ZnO films on the gold surface and hence determine the direction of growth, the dominating orientation with the increase of the gold sub-layer thickness should be the (002) direction. Indeed, the structural data (Fig. 1) have shown that XRD peaks of ZnO films are shifted and narrowed, which confirms the improvement of the crystalline structure.

Analysis of the absorption spectra and spectroscopic ellipsometry data has shown that ultra-thin gold layers have a strong influence on the optical response of Au/ZnO nanostructures. In both cases, similar spectral dependencies of the localized plasmon peak were observed. The red shift of LSPR peaks in the Au and Au/ZnO absorption spectra could be associated with size effects based on the Au grain size growth during the formation of Au nanolayers and the ZnO layer on the top.<sup>12,13,34</sup>

It is well known that the LSPR peak in pure Au nanostructures is normally located in the range of 450–580 nm, depending on the grain size and the surrounding media.<sup>12,13,34</sup> The LSPR peak positions in Au/ZnO samples were red-shifted by 30–60 nm in comparison to that of bare Au nanolayers. The observed phenomenon could be related to the ZnO upper layer.

Regression analysis of ellipsometric parameters (Fig. 3a–c) revealed the different optical responses according to various dispersion laws in the case of Au island-like films (Fig. 3b and c) and Au 30 nm, more like bulk (Fig. 3a). The obtained dispersion spectra of  $n(\lambda)$  and  $k(\lambda)$  for various thicknesses of gold films have been shown to possess a typical dielectric behaviour for 2.5–15 nm (Fig. 3b and c) and the transformation to the metallic type for the 30 nm thick gold layer (Fig. 3a).<sup>35</sup> The Drude dispersion function of the 30 nm thick gold film changes to the Lorentz type peaks of localized plasmon absorption for the thin gold films (2.5–15 nm). The red shift of the plasmon absorption peak in  $k(\lambda)$  (Fig. 3c) indicates the changes in the gold film structure: from separate island-like films for 2.5–5 nm thick gold to an increase of the crystallite sizes and the formation of gold clusters on a Si substrate for 10–15 nm thick gold.

Analysis of ellipsometric data of Au/ZnO nanostructures has shown that, generally, a similar optical dispersion of the Au layers in hybrid systems of different structures indicates that the accepted multilayer model is valid for analysis of complex systems containing metal island-like films.<sup>22</sup> Regression analysis results of the optical dispersion of 50 nm thick ZnO layers are presented in Fig. 4c and compared with reported data in the literature (J.A. Woollam CompleteEASE database, version 4.13). The red shift of absorption line from 356 nm to 375 nm (Fig. 4c) is clearly seen for ZnO films deposited on the Au island-like films in comparison with reference data. Such behavior of absorption line could be related to excitonic peak shift to lower energies in ZnO.<sup>36</sup>

Numerous publications were dedicated for the study of the dependence of the effective refractive index of Au nanolayers to the structural properties and the coverage of the surface area.<sup>33,37</sup> Different behaviors of the complex dielectric function

for Au nanolayers from the cluster-to-bulk morphology were observed.<sup>33</sup> Chen *et al.* described changes of the refractive index and extinction coefficient of Au nanoparticles, which were adsorbed onto the Si wafer, in relation to the surface coating of the adsorbed particles.<sup>37</sup> As a rule, the Maxwell–Garnett or the Bruggemann effective medium model for calculations was usually applied to determine the effective refractive index. The obtained values of the refractive index increased in the range of 0.1–0.6 surface coating ratio, reached the maximum at 0.65 and then monotonically decreased. It should be noted that regression analysis of pure Au nanolayers and Au/ZnO hybrid structures showed that the roughness of Au films play an important role in the excitation conditions of LSPR; moreover these optical features strongly influence the dispersion function and reflect structural changes of gold nanolayers. Taking into account the behavior of the complex refractive index determined from the regression analysis of SE for 2.5–30 nm thick Au layers and the effects reported by Wang *et al.*,<sup>33</sup> Chen *et al.*<sup>37</sup> and Zhang *et al.*,<sup>32</sup> it should be concluded that the optical response of bare Au nanolayers and those with the ZnO coating demonstrate cluster-to-thin film transition when the Au layer thickness increases to more than 15 nm.

The photoluminescence (PL) spectra of the Au/ZnO nanostructures and pure ZnO layer are presented in Fig. 5. The peaks observed at 381–382 nm correspond to free exciton emission (FX<sup>0</sup>).<sup>6,7,29</sup> The peaks in the visible spectral range at 540–660 nm correspond to defects based on oxygen and zinc vacancy levels.<sup>6,7,29</sup> A pure ZnO layer of 50 nm thickness shows a weak UV peak and a relatively strong peak for the visible part of spectrum. However, for Au/ZnO nanostructures of 2.5–10 nm the strong enhancement of the UV peak and the quenching of the visible part of spectra are clearly seen; meanwhile for samples with 15 and 30 nm gold thickness UV enhancement was not observed. Such a behavior of optical response strongly correlates with the ability of the gold layer to efficiently excite the localized plasmon resonance. Therefore the UV peaks were weak for samples with 15 and 30 nm gold layers where LSPR was strongly decreased or fully disappeared.

The fact that the presence of the Au/ZnO interface resulted in the increase of UV and the quenching of the Vis-emission was reported in numerous publications.<sup>20–22,32,38,39,40</sup> It is known that the Schottky barrier is formed at the interface between Au and ZnO. The enhancement of UV emission is explained by electron transfer from the defect states to the conduction band of ZnO layers through the interaction with localized surface plasmons.<sup>32,40</sup> This leads to an increase of electrons density in higher energy states of Au layer and further transfer of those electrons to the conduction band of ZnO leads to the increase of the UV emission.<sup>38,39</sup> Meanwhile the PL peak in the Vis range reduced or almost disappeared due to electron non-radiative transition from defect states to the Fermi level of gold. Such a transition is energetically more probable than the electron transition to the valence band of ZnO (visible PL spectra).

In our study the intensity of the spectral feature was dependent on the gold layer thickness and hence on the surface area covered by gold islands on the Si substrate. The precise determination of optical dispersion dependencies of the Au

layers *vs.* their thickness changes should be taken into account for the characterization of the photoluminescence features in Au/ZnO nanostructures. The structure of the Au layers strongly affects not only the photoluminescence spectra, but also the complex refractive index of the same ZnO layer (Fig. 4c).

The change in the photoluminescence response clearly demonstrates the extreme sensitivity of the system to the composition and the structure, in particular, to the presence of thin gold layers, which increases the UV PL peak intensity and quenches the PL in the visible wavelength range. In order to apply the hybrid structure under consideration in various optical applications, such as LED or efficient solid state emitters, the dispersion of optical parameters of the components should be optimized, taking into account a particular target.

The proposed technological approach allows the tailoring of the optical and structural properties of ZnO and Au nanolayers, which could be used for the development of novel hybrid nanostructure based LSPR and photoluminescence phenomena.

## E Conclusions

Optical and structural experiments have been carried out on Si/ZnO structures modified with ultra-thin gold layers of different thicknesses. The thin gold layers between Si substrate and ZnO layer strongly influence the photoluminescence properties of Si/Au/ZnO nanostructures. However, the optical response of metal–semiconductor nanostructures was successfully analyzed in the multilayer model taking into account the contribution of thin gold layers optical dispersion. It should be noted that analysis of optical features of the system have shown that slight changes of localized plasmon absorption peaks in spectra have noticeable contribution to complex refractive index of gold film and, as a result, this leads to strong enhancement of UV PL peak in ZnO layer.

In conclusion, we have summarized that through the changes of structural properties of thin gold layer between Si substrate and ZnO layer, we can tune the optical dispersion of each layer and due to that, the control of ZnO PL spectra enhancement and quenching in UV-Vis wavelengths region is possible.

## Authors contribution

A.AC., M.B., P.M.: experiment and characterization of Physical Vapor deposition and atomic layer deposition; Z. B., I. B., L. M., S. T., A. R.: AFM, spectroscopic ellipsometry measurement and FTIR; R. V., Z. G., A. Z., V. V., V. S., D. E.: transmittance and photoluminescence (PL) measurement. M.B., R. V., Z. B. and S. T.: Design study, data interpretation, wrote the paper.

## Acknowledgements

The research was supported by Fotonika –LV (FP7-Reg Pot-2011-1, contract no. 285912) and BIOSENSORS-AGRICULT (FP7-PEOPLE-2012-IRSES, contract no. 318520) projects. This work was partially supported by PHC GILBERT 2015 (Project no. 32978PG).

This research was funded as well by a grant (No. TAP LZ-3/2015) from the Research Council of Lithuania.

## Notes and references

- 1 N. Gogurla, A. K. Sinha, S. Santra, S. Manna and S. K. Ray, *Sci. Rep.*, 2014, **4**, 6483.
- 2 A. A. Chaaya, M. Bechelany, S. Balme and P. Miele, *J. Mater. Chem. A*, 2014, **2**, 20650–20658.
- 3 Y.-S. Choi, J.-W. Kang, H. Dae-Kue and S.-J. Park, *IEEE Trans. Electron Devices*, 2010, **57**, 26–41.
- 4 M. Jędrzejewska-Szczerska, P. Wierzbza, A. A. Chaaya, M. Bechelany, P. Miele, R. Viter, A. Mazikowski, K. Karpienko and M. Wróbel, *Sens. Actuators, A*, 2015, **221**, 88–94.
- 5 G. Sberveglieri, C. Baratto, E. Comini, G. Faglia, M. Ferroni, A. Ponzoni and A. Vomiero, *Sens. Actuators, B*, 2007, **121**, 208–213.
- 6 R. Viter, V. Khranovskyy, N. Starodub, Y. Ogorodniichuk, S. Gevelyuk, Z. Gertnere, N. Poletaev, R. Yakimova, D. Erts, V. Smyntyna and A. Ubelis, *IEEE Sens. J.*, 2014, **14**, 2028–2034.
- 7 A. Abou Chaaya, R. Viter, M. Bechelany, Z. Alute, D. Erts, A. Zalesskaya, K. Kovalevskis, V. Rouessac, V. Smyntyna and P. Miele, *Beilstein J. Nanotechnol.*, 2013, **4**, 690–698.
- 8 Ü. Özgür, Y. I. Alivov, C. Liu, A. Teke, M. A. Reshchikov, S. Doğan, V. Avrutin, S.-J. Cho and H. Morkoç, *J. Appl. Phys.*, 2005, **98**, 041301.
- 9 M. Bechelany, P. Brodard, J. Elias, A. Brioude, J. Michler and L. Philippe, *Langmuir*, 2010, **26**, 14364–14371.
- 10 M. Bechelany, P. Brodard, L. Philippe and J. Michler, *Nanotechnology*, 2009, **20**, 455302.
- 11 P. Brodard, M. Bechelany, L. Philippe and J. Michler, *J. Raman Spectrosc.*, 2012, **43**, 745–749.
- 12 M. M. Alvarez, J. T. Khoury, T. G. Schaaff, M. N. Shafigullin, I. Vezmar and R. L. Whetten, *J. Phys. Chem. B*, 1997, **101**, 3706–3712.
- 13 T. A. El-Brollossy, T. Abdallah, M. B. Mohamed, S. Abdallah, K. Easawi, S. Negm and H. Talaat, *Eur. Phys. J.: Spec. Top.*, 2008, **153**, 361–364.
- 14 M. Lepoitevin, M. Lemouel, M. Bechelany, J.-M. Janot and S. Balme, *Microchim. Acta*, 2014, 1–7.
- 15 W. X. Jing, H. Qi, L. L. Niu, Z. D. Jiang, B. Wang, L. J. Chen, F. Zhou and Y. L. Zhao, *Phys. E*, 2014, **56**, 196–204.
- 16 C. Sandoval, O. Marin, S. Real, D. Comedi and M. Tirado, *Mater. Sci. Eng. B*, 2014, **187**, 21–25.
- 17 T. Chen, G. Z. Xing, Z. Zhang, H. Y. Chen and T. Wu, *Nanotechnology*, 2008, **19**, 435711.
- 18 C. W. Cheng, E. J. Sie, B. Liu, C. H. A. Huan, T. C. Sum, H. D. Sun and H. J. Fan, *Appl. Phys. Lett.*, 2010, **96**, 071107.
- 19 S. T. Kochuveedu, J. H. Oh, Y. R. Do and D. H. Kim, *Chem. – Eur. J.*, 2012, **18**, 7467–7472.
- 20 S. Park, Y. Mun, S. An, W. In Lee and C. Lee, *J. Lumin.*, 2014, **147**, 5–8.
- 21 Y. Zeng, Y. Zhao and Y. Jiang, *J. Alloys Compd.*, 2015, **625**, 175–181.
- 22 M. D. L. Ruiz Peralta, U. Pal and R. Sanchez Zeferino, *ACS Appl. Mater. Interfaces*, 2012, **4**, 4807–4816.
- 23 L. Su and N. Qin, *Ceram. Int.*, 2015, **41**, 2673–2679.
- 24 D. Y. Lei and H. C. Ong, *Appl. Phys. Lett.*, 2007, **91**, 021112.
- 25 H. Fujiwara, *Spectroscopic Ellipsometry*, John Wiley & Sons, Ltd, 2007, pp. 81–146.
- 26 J. Elias, M. Bechelany, I. Utke, R. Erni, D. Hosseini, J. Michler and L. Philippe, *Nano Energy*, 2012, **1**, 696–705.
- 27 D. Selloum, A. A. Chaaya, M. Bechelany, V. Rouessac, P. Miele and S. Tingry, *J. Mater. Chem. A*, 2014, **2**, 2794–2800.
- 28 M. Nasr, A. Abou Chaaya, N. Abboud, M. Bechelany, R. Viter, C. Eid, A. Khoury and P. Miele, *Superlattices Microstruct.*, 2015, **77**, 18–24.
- 29 A. A. Chaaya, R. Viter, I. Baleviciute, M. Bechelany, A. Ramanavicius, Z. Gertnere, D. Erts, V. Smyntyna and P. Miele, *J. Phys. Chem. C*, 2014, **118**, 3811–3819.
- 30 Z. Balevicius, R. Drevinskas, M. Dapkus, G. J. Babonas, A. Ramanaviciene and A. Ramanavicius, *Thin Solid Films*, 2011, **519**, 2959–2962.
- 31 Z. Balevicius, V. Vaicikauskas and G. J. Babonas, *Appl. Surf. Sci.*, 2009, **256**, 640–644.
- 32 Y. Zhang, X. Li and X. Ren, *Opt. Express*, 2009, **17**, 8735–8740.
- 33 X. Wang, K.-p. Chen, M. Zhao and D. D. Nolte, *Opt. Express*, 2010, **18**, 24859–24867.
- 34 L. Wang, Y. Sun, J. Wang, J. Wang, A. Yu, H. Zhang and D. Song, *J. Colloid Interface Sci.*, 2010, **351**, 392–397.
- 35 T. W. H. Oates, H. Wormeester and H. Arwin, *Prog. Surf. Sci.*, 2011, **86**, 328–376.
- 36 R. Ghosh, D. Basak and S. Fujihara, *J. Appl. Phys.*, 2004, **96**, 2689–2692.
- 37 M. Chen and R. G. Horn, *J. Colloid Interface Sci.*, 2007, **315**, 814–817.
- 38 D. Sahu, N. R. Panda, B. S. Acharya and A. K. Panda, *Opt. Mater.*, 2014, **36**, 1402–1407.
- 39 T. Singh, D. K. Pandya and R. Singh, *Thin Solid Films*, 2012, **520**, 4646–4649.
- 40 J. Huang, K. H. P. Tung, L. Deng, N. Xiang, J. Dong, A. J. Danner and J. Teng, *Opt. Mater. Express*, 2013, **3**, 2003–2011.